Chapter 4

Testing the warmness of dark matter

In this chapter, we investigate two extended properties of DM: a possible time dependence of the EoS of DM via CPL parametrization, and the constant non-null sound speed $\hat{c}^2_{\rm s,dm}$. In the first study, we investigate these extended DM properties with a cosmological constant type DE. We call this model as ΛWDM. In our second study, we investigate extended DM properties with the time-varying DE EoS via CPL parametrization. We call this model as VWDM. We analyze both the models on top of the base ΛCDM model by using the data from Planck-CMB, BAO, and the Hubble constant measurement from HST. Our aim is to find new and robust constraints on the extended parameters of the models and to see how these extended parameters affect other parameters of the standard ΛCDM model. In our first study, we also estimate the warmness of DM particles as well as their mass scale. We compare our results of the first study with previous similar studies in the literature. In addition, we have also presented observational constraints on the standard ΛCDM model with all the data sets under consideration, for comparison purposes. The research work presented in this chapter is carried out in the research papers [153, 154].

4.1 Introduction

In the standard ΛCDM model, the major component "cosmological constant" (Λ) is associated with DE fluid whereas the CDM is considered as pressureless, non-interacting (except gravitationally) perfect fluid having zero EoS parameter as well as zero sound speed and zero viscosity. The consideration of CDM in the standard model leads to many small scale problems. For instance, the observed halo properties differ from the predictions of the standard ΛCDM model which might be an indication of DM being more complex than simply CDM. Many observed halo density profiles have cores in their centers rather than cusps [36], and some have substructures [155] that are at odds with the standard ΛCDM simulations. Also, the low observed mass function of small halos seems to be in a serious disagreement with the results from the standard ΛCDM simulations [38, 156]. The proposed candidate, which may alleviate many of small scale issues, is the warm DM (WDM), and it is not distinguishable from CDM on larger scales. Therefore, the investigation of the precise nature of DM is important and worthwhile in modern cosmology. Several attempts have been done in the literature to understand the general properties such as mass, interaction cross-section, spin, etc. and precise nature of DM by investigating its generalized or extended properties. In [157], it is claimed that the warmness of DM can successfully reproduce the astronomical observations from small to large scales. To test the warmness of DM, the author in [158] has investigated the EoS parameter of DM using CMB, SNe Ia, and LSS data with zero adiabatic sound speed and no entropy production. The authors in [159] and [160] have constrained the EoS of DM by combining kinematic and gravitational lensing data. The warmness of DM has also been investigated in interacting and non-interacting scenarios of DM and DE by assuming constant EoS of both DM and DE in [161] and [162]. Many models of DM and DE have been constrained by assuming constant as well as variable EoS parameters of DM and DE in [163], where the authors have found that warmness of DM is not favored over coldness in the light of data from CMB, SNe Ia, and BAO. The author [152] have investigated the fluid perspective of DM and DE via variable EoS parameter of both, and found no significant deviation

from the CDM scenario, but obtained tighter constraints on EoS of DM in comparison to previous similar studies [164, 165]. In most of the above-mentioned works, the authors have focused only on constraining the EoS parameter of DM by considering it, either as a constant or time-varying in different mathematical forms. The other generalized properties, like, sound speed and viscosity have been considered to be zero, either for simplicity or to avoid a large number of model parameters. Recently, an extensive investigation of the generalized properties of DM: EoS parameter, sound speed and viscosity (initially proposed in [166]) are discussed in detail, in [167]. Next, in [168] the authors have found strong observational constraints on generalized DM parameters with recent observational data sets. Similar constraints on generalized DM properties have also been found in [169]. Most recently, generalized DM properties have been investigated in [170] to reconcile the tension between Planck-CMB and weak lensing observations. The authors in [171] have tested the inverse cosmic volume law for DM by allowing its EoS to vary independently in eight redshift bins from $z = 10^5$ to $z = 0$ by using the latest observational data, and found no evidence for non-zero EoS parameter in any of the eight redshift bins. In the light of above literature, we are motivated to place robust and accurate constraints on some extended properties of DM such as its EoS parameter and sound speed, which are helpful to characterize the physical nature of DM. Recently, the generalized DM parameters have been constrained in [168], where all the parameters are taken as constant. But, there is no reason for the EoS of DM to be a constant, it could be a time-varying as well. Thus, here in our first study, we consider a time-dependent EoS and a constant sound speed of DM whereas viscosity is taken as zero (to avoid a large number of parameters in the model) with cosmological constant type DE. In the second study, a variable DE EoS is taken via CPL parametrization whereas DM is assumed as in first case. We also use same set of data combination for the second study.

4.2 Model with extended properties of dark matter

We consider FLRW Universe, where the background expansion is governed by the so-called Friedmann equations (in the units $c = 1$):

$$3H^2 = 8\pi G \sum_i \rho_i, \tag{4.1}$$

$$2\frac{\mathrm{d}H}{\mathrm{d}t} + 3H^2 = -8\pi G \sum_i P_i, \tag{4.2}$$

where $H = \frac{1}{a}\frac{da}{dt}$ is the Hubble parameter with a being the scale factor of the Universe; t is the cosmic time, and G is the Newton's gravitational constant. Further, ρ_i and P_i are the energy density and pressure of the ith species, where the label i runs over the components $i = \gamma, \nu, b, \mathrm{dm}, \Lambda$, representing photons, neutrinos, baryons, DM and cosmological constant, respectively. Here, we relax the condition that entire DM is purely a pressureless, non-relativistic component. For this, we assume, in principle, that EoS of the DM has a temporal dependence through the cosmic evolution. In order to quantify that we choose the functional form of the CPL parametrization [149, 150] for the EoS of the DM, given by

$$w_{\mathrm{dm}}(a) = w_{\mathrm{dm0}} + w_{\mathrm{dm1}}(1 - a), \tag{4.3}$$

where w_{dm0} and w_{dm1} are free parameters (constants) to be fixed by observations. For $w_{\mathrm{dm0}} = w_{\mathrm{dm1}} = 0$, we recover $w_{\mathrm{dm}} = 0$, the EoS parameter of CDM. We assume that DM is described by a perfect fluid, and as usual quantified by the energy-momentum tensor with density ρ and isotropic pressure p: $T_{\mu\nu} = (\rho + p)u_\mu u_\nu + p g_{\mu\nu}$, where we have disregarded possible anisotropic stress tensor contribution. It is well known that anisotropic stress vanishes for perfect fluids or minimally coupled scalar fields. Taking $p_{\mathrm{dm}} = w_{\mathrm{dm}}\rho_{\mathrm{dm}}$ and the conservation law $\nabla_\mu T^{\mu\nu} = 0$, we have

$$\dot{\rho}_{\mathrm{dm}} + 3H[1 + w_{\mathrm{dm}}(a)]\rho_{\mathrm{dm}} = 0. \tag{4.4}$$

By using CPL parametrization 4.3 for EoS of DM and the conservation eq. 4.4, the evolution of DM density is given by,

$$\rho_{\rm dm} = \rho_{\rm dm0}\, a^{-3(1+w_{\rm dm0}+w_{\rm dm1})}\, e^{-3w_{\rm dm1}(1-a)}. \tag{4.5}$$

At perturbative level, we work in the conformal Newtonian gauge where the perturbed FLRW metric takes the form

$$\mathrm{d}s^2 = a^2(\tau)\Big[-(1+2\psi)\mathrm{d}\tau^2 + (1-2\phi)\mathrm{d}\vec{r}^2\Big], \tag{4.6}$$

where ϕ and ψ are the metric potentials and $\vec{r}$ represents the three spatial coordinates. In the Fourier space, the first order perturbed part of the conserved stress-energy momentum tensor, i.e., $\delta T^{\mu\nu}_{;\nu} = 0$, leads to the following continuity and Euler equations [31] for DM:

$$\dot{\delta}_{\rm dm} = -(1+w_{\rm dm})(\theta_{\rm dm} - 3\dot{\phi}) - 3\mathcal{H}\left(\frac{\delta p_{\rm dm}}{\delta\rho_{\rm dm}} - w\right)\delta_{\rm dm}, \tag{4.7}$$

$$\begin{aligned}\dot{\theta}_{\rm dm} = -(1-3w_{\rm dm})\mathcal{H}\theta_{\rm dm} - \frac{\dot{w}_{\rm dm}}{1+w_{\rm dm}}\theta_{\rm dm} + k^2\psi \\ + \frac{\delta p_{\rm dm}}{\delta\rho_{\rm dm}}k^2\frac{\delta_{\rm dm}}{1+w_{\rm dm}}.\end{aligned} \tag{4.8}$$

Here, an over dot stands for the conformal time derivative, $\mathcal{H}$ is the conformal Hubble parameter, and k is magnitude of the wavevector $\vec{k}$. Further, $\delta_{\rm dm} = \delta\rho_{\rm dm}/\rho_{\rm dm}$ and $(\rho_{\rm dm} + p_{\rm dm})\theta_{\rm dm} = ik^j\delta T^0_j$ are the relative density and velocity perturbations, respectively, associated with the DM fluid. In a random frame, the quantity $\delta p_{\rm dm}/\delta\rho_{\rm dm}$ can be expressed as [172],

$$\rho^{-1}\delta p_{\rm dm} = \delta_{\rm dm}\hat{c}^2_{\rm s,dm} + 3\mathcal{H}(1+w_{\rm dm})(\hat{c}^2_{\rm s,dm} - c^2_{\rm a,dm})\frac{\theta_{\rm dm}}{k^2}, \tag{4.9}$$

where $\hat{c}_{\rm s,dm}$ represents the sound speed of DM in the rest frame, and $c^2_{\rm a,dm}$ denotes the adiabatic sound speed squared, defined as

$$c^2_{\rm a,dm} = \frac{\dot{p}_{\rm dm}}{\dot{\rho}_{\rm dm}} = w_{\rm dm} - \frac{\dot{w}_{\rm dm}}{3\mathcal{H}(1+w_{\rm dm})}. \tag{4.10}$$

The above two equations allow to recast (4.7) and (4.8) as follows:

$$\begin{aligned}\dot{\delta}_{\rm dm} = -(1+w_{\rm dm})\left(\theta_{\rm dm} - 3\dot{\phi}\right) - 3\mathcal{H}\delta_{\rm dm}(\hat{c}^2_{\rm s,dm} - w_{\rm dm}) \\ -9(1+w_{\rm dm})(\hat{c}^2_{\rm s,dm} - c^2_{\rm a,dm})\mathcal{H}^2\frac{\theta_{\rm dm}}{k^2},\end{aligned} \tag{4.11}$$

$$\dot{\theta}_{\rm dm} = \ -(1-3\hat{c}^2_{\rm s,dm})\mathcal{H}\theta_{\rm dm} + \frac{\hat{c}^2_{\rm s,dm}}{1+w_{\rm dm}}k^2\delta_{\rm dm} + k^2\psi. \tag{4.12}$$

The sound speed of DM describes its micro-scale properties. Here, we consider $\hat{c}^2_{\rm s,dm}$ as a constant model parameter to be fixed by observations. A significant deviation of sound speed from zero in light of cosmological observations can be interpreted as possible evidence for DM to be more complicated than simple CDM.

4.2.1 Results and discussion

Considering the background and perturbation dynamics presented in the previous section, we explore the full parameter space of the cosmological scenario under consideration. The baseline free parameters set of ΛWDM model is, therefore:

$$\mathcal{P}_{\Lambda\rm WDM} = \left\{\omega_{\rm b},\, \omega_{\rm dm},\, \theta_s,\, A_s,\, n_s,\, \tau_{\rm reio},\, w_{\rm dm0},\, w_{\rm dm1},\, \hat{c}^2_{\rm s,dm}\right\},$$

where the first six parameters are the baseline parameters of the ΛCDM model, and the last three are the extended DM properties ($w_{\rm dm0},\, w_{\rm dm1},\, \hat{c}^2_{\rm s,dm}$). To obtain observational constraints on all the model parameters, we use the data from CMB, BAO, and HST measurements in the following four combinations: CMB, CMB + BAO, CMB + HST, and CMB + BAO + HST. We use flat priors on all the free parameters as mention in Table

Table 4.1: Uniform priors on the free parameters of the model under study.

Parameter	Prior
$100\omega_{\rm b}$	[1.8, 2.6]
$\omega_{\rm dm}$	[0.01, 0.99]
$100\theta_s$	[0.5, 2.5]
$\ln[10^{10}A_s]$	[2.7, 4.0]
n_s	[0.9, 1.3]
$\tau_{\rm reio}$	[0.01, 0.8]
$w_{\rm dm0}$	[0, 0.1]
$w_{\rm dm1}$	[0, 0.1]
$\hat{c}^2_{\rm s,dm}$	[0, 0.1]

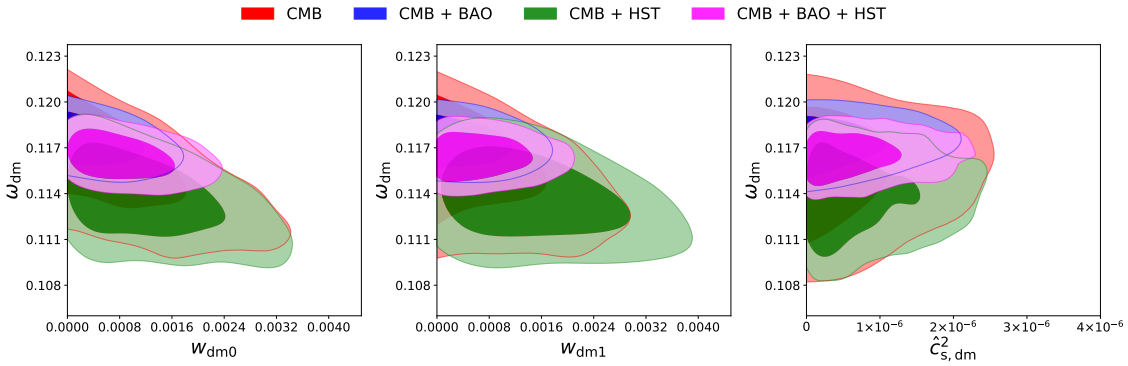

Figure 4.1: Two-dimensional marginalized distributions (68% and 95% CL) of some free parameters of ΛWDM model.

4.1.

We have chosen $w_{\rm dm0} \geq 0$ and $w_{\rm dm1} \geq 0$ in this work, though in the literature some authors have presented constraints allowing negative range of the EoS parameter $w_{\rm dm}$ of DM, but they do not find negative $w_{\rm dm}$ suitable for well-motivated physics. For instance, in [158], it is stated that there is no particle motivation for negative $w_{\rm dm}$. On the other hand, in [152], the constraints on $w_{\rm dm}$ are presented by choosing its positive prior range due to the possible degeneracy with dark energy at the background level. Also, it is demonstrated in [173] that all physical species (baryons, photons, neutrinos, dark matter, etc.) must satisfy certain conditions on their EoS, in order to be stable from thermodynamics point of view, and here the DM fluid satisfies those conditions naturally with

Table 4.2: Constraints on the free parameters and some derived parameters of ΛWDM model for four data combinations. The upper and lower values over the mean value of each parameter denote 68% CL and 95% CL errors. For the parameters: $w_{\rm dm0}$, $w_{\rm dm1}$, and $\hat{c}^2_{\rm s,dm}$, the upper bounds at 95% CL are mentioned. The parameter H_0 is measured in the units of km s^{-1} Mpc^{-1}. The entries in the second row of parameters represent the constraints on the same from standard ΛCDM model. The final row displayed the $\chi^2_{\rm min}$ values.

Parameter	CMB	CMB + BAO	CMB + HST	CMB + BAO + HST
$10^2\omega_{\rm b}$	$2.216^{+0.016+0.033}_{-0.016-0.031}$	$2.217^{+0.015+0.031}_{-0.015-0.029}$	$2.218^{+0.016+0.032}_{-0.016-0.031}$	$2.218^{+0.016+0.032}_{-0.016-0.031}$
	$2.226^{+0.015+0.030}_{-0.015-0.029}$	$2.235^{+0.014+0.027}_{-0.014-0.027}$	$2.238^{+0.015+0.030}_{-0.015-0.029}$	$2.243^{+0.013+0.026}_{-0.013-0.026}$
$\omega_{\rm dm}$	$0.1156^{+0.0029+0.0047}_{-0.0021-0.0051}$	$0.1173^{+0.0011+0.0023}_{-0.0011-0.0022}$	$0.1173^{+0.0020+0.0038}_{-0.0020-0.0038}$	$0.1164^{+0.0011+0.0021}_{-0.0011-0.0021}$
	$0.1193^{+0.0014+0.0029}_{-0.0014-0.0028}$	$0.1181^{+0.0010+0.0020}_{-0.0010-0.0020}$	$0.1179^{+0.0013+0.0027}_{-0.0013-0.0025}$	$0.1173^{+0.0010+0.0020}_{-0.0010-0.0020}$
$100\theta_s$	$1.04166^{+0.00031+0.00059}_{-0.00031-0.00062}$	$1.04171^{+0.00031+0.00062}_{-0.00031-0.00059}$	$1.04166^{+0.00032+0.00063}_{-0.00032-0.00065}$	$1.04172^{+0.00032+0.00063}_{-0.00032-0.00061}$
	$1.04185^{+0.00029+0.00057}_{-0.00029-0.00056}$	$1.04197^{+0.00028+0.00055}_{-0.00028-0.00056}$	$1.04197^{+0.00029+0.00057}_{-0.00029-0.00056}$	$1.04204^{+0.00029+0.00055}_{-0.00029-0.00056}$
$\ln 10^{10} A_s$	$3.089^{+0.027+0.058}_{-0.030-0.053}$	$3.082^{+0.025+0.047}_{-0.025-0.049}$	$3.100^{+0.027+0.051}_{-0.027-0.052}$	$3.084^{+0.026+0.051}_{-0.026-0.052}$
	$3.065^{+0.025+0.048}_{-0.025-0.050}$	$3.077^{+0.023+0.044}_{-0.023-0.045}$	$3.079^{+0.025+0.047}_{-0.025-0.049}$	$3.087^{+0.022+0.045}_{-0.022-0.043}$
n_s	$0.9651^{+0.0049+0.0096}_{-0.0049-0.0093}$	$0.9741^{+0.0045+0.0088}_{-0.0045-0.0085}$	$0.9661^{+0.0045+0.0090}_{-0.0045-0.0089}$	$0.9645^{+0.0045+0.0089}_{-0.0045-0.0088}$
	$0.9647^{+0.0049+0.0099}_{-0.0049-0.0094}$	$0.9680^{+0.0040+0.0078}_{-0.0040-0.0079}$	$0.9684^{+0.0047+0.0090}_{-0.0047-0.0090}$	$0.9701^{+0.0040+0.0080}_{-0.0040-0.0076}$
$\tau_{\rm reio}$	$0.076^{+0.015+0.030}_{-0.015-0.029}$	$0.072^{+0.013+0.025}_{-0.013-0.027}$	$0.080^{+0.014+0.028}_{-0.014-0.027}$	$0.073^{+0.014+0.027}_{-0.014-0.027}$
	$0.066^{+0.014+0.026}_{-0.014-0.028}$	$0.073^{+0.012+0.023}_{-0.012-0.024}$	$0.075^{+0.013+0.026}_{-0.013-0.027}$	$0.079^{+0.012+0.024}_{-0.012-0.023}$
$w_{\rm dm0}$ (95% CL)	$< 2.78 \times 10^{-3}$	$< 1.43 \times 10^{-3}$	$< 2.95 \times 10^{-3}$	$< 1.94 \times 10^{-3}$
$w_{\rm dm1}$ (95% CL)	$< 2.26 \times 10^{-3}$	$< 1.44 \times 10^{-3}$	$< 3.15 \times 10^{-3}$	$< 1.68 \times 10^{-3}$
$\hat{c}^2_{\rm s,dm}$ (95% CL)	$< 2.18 \times 10^{-6}$	$< 1.79 \times 10^{-6}$	$< 2.31 \times 10^{-6}$	$< 1.95 \times 10^{-6}$
$\Omega_{\rm m}$	$0.279^{+0.022+0.036}_{-0.016-0.038}$	$0.292^{+0.008+0.017}_{-0.008-0.016}$	$0.264^{+0.014+0.028}_{-0.014-0.026}$	$0.284^{+0.007+0.015}_{-0.007-0.014}$
	$0.312^{+0.009+0.017}_{-0.009-0.017}$	$0.304^{+0.006+0.012}_{-0.006-0.012}$	$0.303^{+0.007+0.016}_{-0.008-0.014}$	$0.300^{+0.006+0.012}_{-0.006-0.012}$
Ω_Λ	$0.721^{+0.016+0.038}_{-0.022-0.035}$	$0.707^{+0.008+0.016}_{-0.008-0.017}$	$0.736^{+0.014+0.026}_{-0.014-0.028}$	$0.715^{+0.008+0.015}_{-0.008-0.015}$
	$0.688^{+0.009+0.017}_{-0.009-0.017}$	$0.695^{+0.006+0.012}_{-0.006-0.012}$	$0.697^{+0.008+0.014}_{-0.007-0.016}$	$0.700^{+0.006+0.012}_{-0.006-0.012}$
H_0	$70.50^{+1.40+3.60}_{-2.10-3.20}$	$69.26^{+0.73+1.50}_{-0.73-1.40}$	$72.00^{+1.40+2.70}_{-1.40-2.70}$	$69.93^{+0.71+1.40}_{-0.71-1.30}$
	$67.53^{+0.64+1.30}_{-0.64-1.30}$	$68.08^{+0.47+0.91}_{-0.47-0.90}$	$68.18^{+0.59+1.10}_{-0.59-1.20}$	$68.45^{+0.46+0.92}_{-0.46-0.91}$
σ_8	$0.749^{+0.093+0.130}_{-0.050-0.160}$	$0.749^{+0.085+0.110}_{-0.040-0.140}$	$0.747^{+0.110+0.130}_{-0.054-0.170}$	$0.745^{+0.091+0.120}_{-0.049-0.140}$
	$0.817^{+0.009+0.017}_{-0.009-0.017}$	$0.819^{+0.009+0.018}_{-0.009-0.017}$	$0.819^{+0.009+0.017}_{-0.009-0.018}$	$0.820^{+0.008+0.017}_{-0.008-0.016}$
$\chi^2_{\rm min}/2$	6476.21	6481.00	6478.57	6483.41
	6475.32	6481.24	6480.26	6485.36

$w_{\rm dm0} \geq 0$ and $w_{\rm dm1} \geq 0$. Table 4.2 summarizes the observational constraints on the parameters of the ΛWDM model with four combinations of the data sets: CMB, CMB + BAO, CMB + HST, and CMB + BAO + HST. The corresponding ΛCDM constraints are displayed in the second row for each parameter for comparison purposes. The constraints on the three extended DM parameters are given with upper bounds at 95% CL. As expected, we see very tight constraints on these parameters of DM: the constraints on both the EoS parameters $w_{\rm dm0}$ and $w_{\rm dm1}$ of DM are of order 10^{-3} at 95% CL, and the constraint on the sound speed $\hat{c}^2_{\rm s,dm}$ of DM is of the order 10^{-6} at 95% CL, from all the four data combinations. We note that the most tight constraints are imposed by CMB + BAO data where the three parameters $w_{\rm dm0}$, $w_{\rm dm1}$, and $\hat{c}^2_{\rm s,dm}$ are respectively constrained to be less than 1.43×10^{-3}, 1.44×10^{-3}, and 1.79×10^{-6} at 95% CL. From all the data combinations, we find that the constraints on all the three extended parameters of DM are consistent with zero at 95% CL. This shows that the CDM paradigm is consistent with the present observational data used in this study. However, there are some interesting consequences on the standard ΛCDM dynamics via the small corrections of the extended DM parameters within their observed bounds, even if there is no enough statistical evidence to deviate from the CDM paradigm, as we will see in the following. From Figure 4.1, we observe a small negative correlation of the DM EoS parameters $w_{\rm dm0}$ and $w_{\rm dm1}$ with $\omega_{\rm dm}$. It implies that larger values of $w_{\rm dm0}$ and $w_{\rm dm1}$ would correspond to smaller values of $\omega_{\rm dm}$. Consequently, in Table 4.2, we see smaller mean values of $\omega_{\rm dm}$ in comparison to the ΛCDM model, in all four cases of data combinations. Similarly, we notice smaller mean values of $\omega_{\rm b}$ in all cases. Consequently, we find smaller mean values of the derived parameter, $\Omega_{\rm m}$, the fractional matter density and larger mean values of Ω_Λ, the fractional DE density in comparison to the ΛCDM model (see Table 4.2). The derived parameters H_0 and σ_8, representing the present Hubble expansion rate of the Universe and amplitude of present matter density fluctuation in a sphere of the radius of $8h^{-1}$Mpc, respectively, are also affected significantly due to the inception of the extended DM parameters. It can be seen from Table 4.2 that the variability of EoS of DM provides the higher mean values of Hubble constant (as compared to ΛCDM). We have $H_0 = 70.50^{+1.40}_{-2.10}$ km s^{-1}Mpc^{-1} at

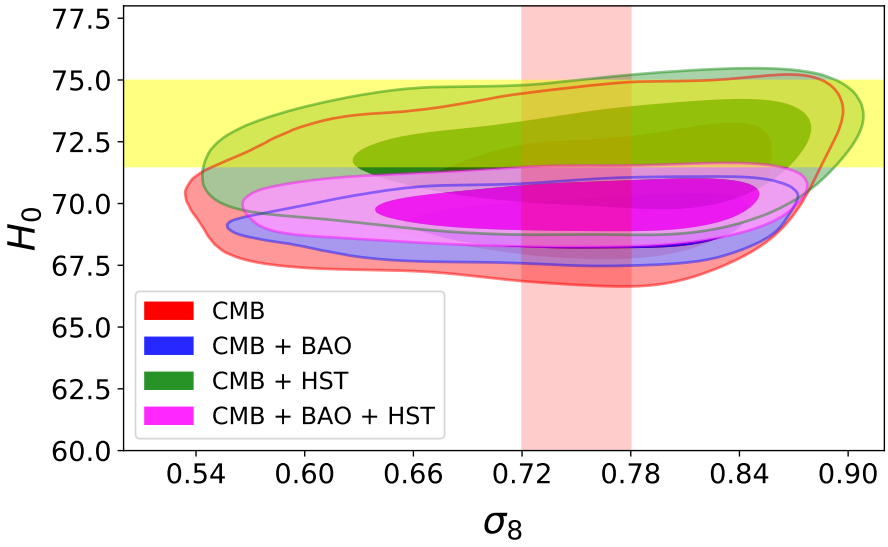

Figure 4.2: Parametric space in the plane $H_0 - \sigma_8$ for ΛWDM from four different data combinations. The horizontal yellow band corresponds to $H_0 = 73.24 \pm 1.74$ km s^{-1} Mpc^{-1} whereas the vertical light red band corresponds to $\sigma_8 = 0.75 \pm 0.03$.

68% CL from Planck-CMB data alone. The inclusion of BAO data yields a slightly lower mean value, $H_0 = 69.26 \pm 0.73$ km s^{-1}Mpc^{-1} at 68% CL with significantly small errors which are Gaussian in nature. It is worthy to mention that due to the less DM abundance (effect of varying DM EoS) as compared to the ΛCDM model, we have higher mean values of Hubble constant even without using HST prior. The constraints presented here on H_0 from CMB and CMB + BAO data combinations are stronger than the constraints obtained in a similar analysis [168] with the same data combinations, where a constant EoS of DM was assumed. The inclusion of HST prior in analysis significantly improves the constraints to $H_0 = 72.00 \pm 1.40$ km s^{-1}Mpc^{-1} at 68% CL, favoring locally measured value of Hubble constant. The constraint with the combined analysis: CMB + BAO + HST, gives $H_0 = 69.93 \pm 0.71$ km s^{-1}Mpc^{-1} at 68% CL which is almost same as with CMB + BAO combination. Also, see Figure 4.2, which shows the parametric space in the plane H_0 - σ_8 for ΛWDM model from the four data combinations. We see that the confidence region for the combination CMB + BAO + HST is almost overlapped with the region from CMB + BAO with a little shift in the mean value of H_0 to the higher side. Thus, the ΛWDM model mildly favors the value of Hubble constant from the local

measurement. We also observe that the parameter H_0 is positively correlated with both the EoS parameters of DM as can be seen in Figure 4.3.

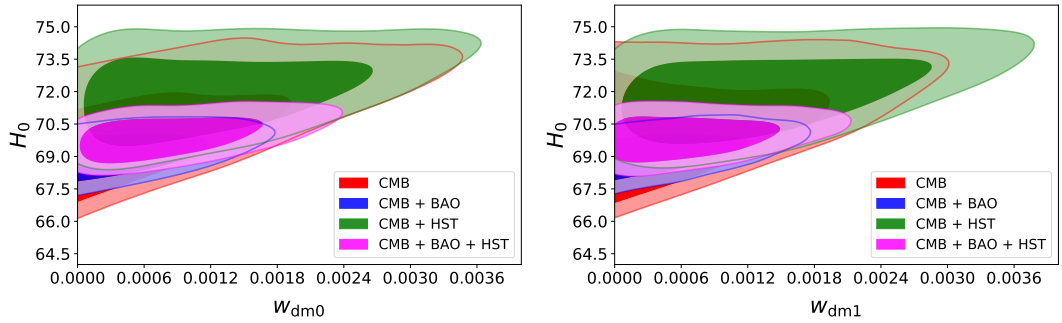

Figure 4.3: Two-dimensional marginalized distributions (68% and 95% CL) of H_0 vs EoS parameters, $w_{\rm dm0}$ and $w_{\rm dm1}$ of DM for ΛWDM model.

The sound speed of DM has a strong degeneracy with the derived parameter σ_8. This is due to the fact that this parameter sufficiently reduces the growth of matter density fluctuations on the length scale below the diffusion length scale [168]. The amplitude of this matter density fluctuation is characterized by σ_8, resulting in a strong degeneracy between this parameter and $\hat{c}^2_{\rm s,dm}$. Figure 4.4 represents the parametric space in the plane $\hat{c}^2_{\rm s,dm}$ - σ_8 with all the four data combinations where we can see that $\hat{c}^2_{\rm s,dm}$ is negatively correlated with σ_8. In Table 4.2, we see lower mean values of σ_8 with all the data combinations but with large errors in each case (compared to the ΛCDM model). These large errors are due to the strong degeneracy between $\hat{c}^2_{\rm s,dm}$ and σ_8. Thus, the presence of the sound speed of DM provides significantly lower mean values of σ_8 consistent with LSS observations. One can also see from Figure 4.2 that the vertical red band, representing the range of σ_8 measured by LSS observations [174], passes through the central region of each contour. From Table 4.2, we notice in general that the inclusion of BAO data significantly tightens the constraints on model parameters whereas the addition of HST prior does not do so. The addition of HST prior to CMB data yields higher mean value of H_0 consistent with the local measurement in the ΛWDM model but not in ΛCDM model. Also, we observe higher mean values of H_0 with other three data combinations in comparison to the ΛCDM. Thus, the underlying ΛWDM model equipped with significant

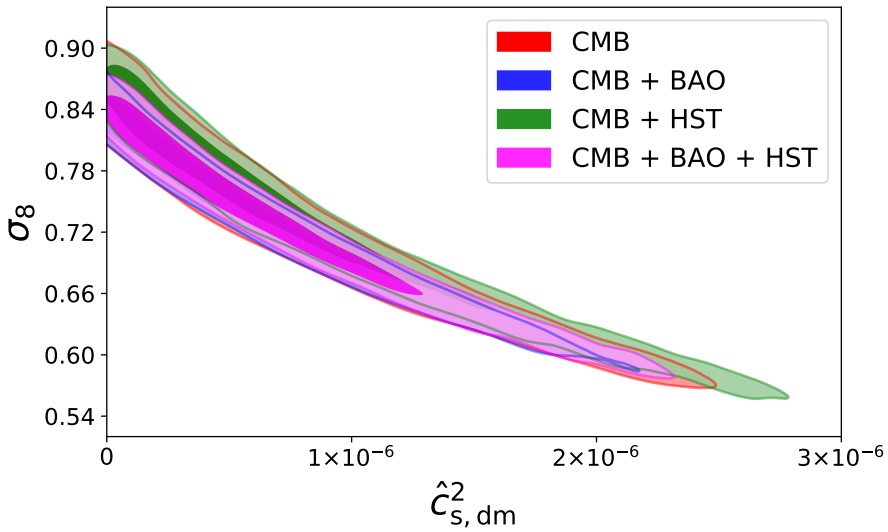

Figure 4.4: Parametric space in the plane $\hat{c}^2_{\rm s,dm} - \sigma_8$ with all data combinations.

positive values of the extended DM parameters might reconcile the H_0 tension.

4.2.2 Estimating the warmness

Without loss of generality, the warmness of DM particles can be estimated by its dynamic character determined by $w_{\rm dm}(a)$. Relaxing the condition $w_{\rm dm} \equiv 0$ and going beyond the non-relativistic limit, we can write

$$w_{\rm dm} \equiv \frac{p_{\rm dm}}{\rho_{\rm dm}} \simeq \frac{T_{\rm dm}}{m_{\rm dm}}, \tag{4.13}$$

where $T_{\rm dm}$ is the DM temperature [175]. Assuming that DM particles interact with other species only gravitationally, we have $T_{\rm dm} = T_{\rm dm0}\ a^{-2}$, where $T_{\rm dm0}$ is the temperature of DM today. Further,

$$T_{\rm dm0} = w_{\rm dm0}\ m_{\rm dm}. \tag{4.14}$$

Thus, from our estimates of $w_{\rm dm0}$, and for a given $m_{\rm dm}$ scale, $T_{\rm dm0}$ can be easily calculated. Within the minimal ΛCDM model, DM particles are assumed to be cold in the strict non-relativistic limit $T_{\rm dm}/m_{\rm dm} \longrightarrow 0$. Thus, we can think of a possible deviation from this limit as a test for the warmness of DM particles. On the other hand, the relativistic limit (for a possible hot species) is determined by $T_{\rm dm}/m_{\rm dm} \gg 1$. Thus, the warm

species must lie between these limits, and here we can quantify it by measuring $w_{\rm dm}(a)$. For any possible evidence of $w_{\rm dm}(a) \neq 0$, we can relax the condition that DM is purely cold, with associated background temperature today given by eq. (4.14), quantifying its warmness. In order to quantify the warmness precisely, we need to determine $m_{\rm dm}$ as required in eq. (4.14). Following standard procedures, the fitting formula from Boltzmann code calculations for the free-streaming on matter distribution is given by a relative transfer function [176]:

$$T_{\rm wdm} = \left[\frac{P_{\rm wdm}(k)}{P_{\rm cdm}(k)}\right]^{1/2} = [1 + (\alpha k)^{2.24}]^{-4.46}, \tag{4.15}$$

where the parameter α is given by

$$\alpha = 0.049\Big(\frac{m_{\rm dm}}{\rm keV}\Big)^{-1.11}\Big(\frac{\Omega_{\rm dm}}{0.25}\Big)^{0.11}\Big(\frac{h}{0.7}\Big)^{1.22} h^{-1}{\rm Mpc}. \tag{4.16}$$

This fitting function applies to the case of thermal relics, and we use it to estimate $m_{\rm dm}$ values. For example, let us choose $\alpha = 0.1h^{-1}$ Mpc [177], though, in general, α should be fit together with other free parameters of the model baseline during the MCMC analysis. Certainly it can bias the results since possible larger α values can lead to smaller borders on $m_{\rm dm}$. But, here, we keep this α upper value for qualitative estimates. Also, we do not assume corrections on non-linear scale, where warm DM properties should manifest significantly, beyond the default modeling implemented in CLASS code. Thus, taking the above mentioned value of α to estimate $m_{\rm dm}$ seems reasonable for simple and qualitative lower bound estimate of $m_{\rm dm}$. In Table 4.3, we summarize the corresponding lower bound on DM mass for all considered data combinations. The estimates on $m_{\rm dm}$ are simply made by direct substitution of the best-fit mean values of the parameters from our analyzes in eq. (4.16). For all data combinations, we notice that $m_{\rm dm} > 0.5$ keV, thus compatible with the Tremaine-Gunn bound [178], that allows structure formation. The authors in [179] have constrained the mass of a thermal warm DM particle (assuming to account for all the DM content, like here) to be $m_{\rm dm} > 0.75$ keV. We see that we have

Table 4.3: Lower bounds on DM mass $m_{\rm dm}$ in the units of keV from four data combinations.

Data	ΛWDM
CMB	0.526
CMB + BAO	0.519
CMB + HST	0.537
CMB + BAO + HST	0.526

also deduced the $m_{\rm dm}$ values in the same order of magnitude. Other borders on warm DM are discussed in [180–188]. Now, an estimate on the warmness of DM can easily be obtained by evaluating the DM temperature today, $T_{\rm dm0}$, using eq. (4.14), and also the evolution DM temperature with the cosmic time, given by $T_{\rm dm}(a) = T_{\rm dm0}\, a^{-2}$.

4.2.3 Comparison with previous studies

The DM EoS parameter has been constrained by many authors in the literature as mentioned in the introduction. Constant EoS of DM has been constrained in [158] by using CMB, SNe Ia, and LSS data: $w_{\rm dm0} < \mathcal{O}(10^{-3})$ at 99.7% CL, assuming vanishing adiabatic sound speed. The authors in [164] have placed the constraints: $w_{\rm dm0} < \mathcal{O}(10^{-2})$ at 95% CL from WMAP alone, which is weaker constraint by an order of magnitude on $w_{\rm dm0}$ at 95% CL found in the present work. In addition, they have found that combining CMB data with SNe Ia, SDSS and HST improves the constraint: $w_{\rm dm0} < \mathcal{O}(10^{-3})$ at 95% CL. The authors in [165] have constrained the EoS of DM by using Planck 2013, BAO, SNe Ia and found $w_{\rm dm0} < \mathcal{O}(10^{-3})$ at 99.7% CL. They have also examined the effect of WIGGLEz measurement of the matter power spectrum, and found that it has a small effect on $w_{\rm dm0}$, and bound is still of order 10^{-3} at 99.7% CL. In [168], the generalized DM parameters: the EoS, sound speed, and viscosity ($c^2_{\rm vis,dm}$) (all are taken as constant) have been constrained by using the data from Planck-2015 together with BAO and HST. They have found the constraints: $w_{\rm dm0} < \mathcal{O}(10^{-3})$ and $\hat{c}^2_{\rm s,dm}$, $c^2_{\rm vis,dm} < \mathcal{O}(10^{-6})$, all at 99.7% CL. In the present work, we have observed that allowing a variable EoS DM provides significantly tighter upper bounds on parameter $w_{\rm dm0}$ than those found in [168], where a constant EoS of DM was assumed. For instance, the tightest upper bound found

in [168] is $w_{\rm dm0} < 2.38 \times 10^{-3}$ at 99.7% CL with the combination: CMB + BAO. In our case, the tightest upper bound is $w_{\rm dm0} < 1.80 \times 10^{-3}$ at 99% CL with same data combination: CMB + BAO. Similarly, with other data combinations, significantly tighter upper bounds on $w_{\rm dm0}$ at 95% CL (also 99% CL) are found as compared to the bounds found by [168]. Authors in [169] have also found similar constraints on extended DM parameters (assuming all constants) by using the data from Planck including polarization with geometric probes from SNe Ia and BAO. The constraints in both the above-mentioned works are in good agreement with our constraints on extended DM parameters. It is important to mention that the present work differs from both [168] and [169] in the fact that they have considered constant EoS of DM together with non-zero viscosity. In the present work, we have considered a time-varying EoS and zero viscosity of DM. Recently, [170] constrained a model with constant EoS and sound speed of DM with zero viscosity and found: $w_{\rm dm0} < \mathcal{O}(10^{-3})$ and $\hat{c}^2_{\rm s,dm} < \mathcal{O}(10^{-6})$, both at 68% CL by using the data combination: CMB + SNe Ia + BAO. In addition, they have also shown that the photometric Euclid survey placed nice constraints on all parameters, in particular, a very strong constraint on the sound speed of DM. The EoS of DM has recently been constrained in [171] by allowing it to vary in eight redshift bins from $z = 10^5$ to present time ($z = 0$), assuming sound speed and viscosity equal to zero, and found that EoS of DM does not deviate significantly from the null value at any time. In short, as expected, there are small corrections on the extended DM parameters $w_{\rm dm0}$, $w_{\rm dm1}$ and $\hat{c}^2_{\rm s,dm}$ in our results in line with the literature. The temporal dependence of $w_{\rm dm}$ in our work is quantified by $w_{\rm dm1}$, and our analysis is a null test of the $w_{\rm dm} = \rm constant$ case in the literature via the CPL parameterization of $w_{\rm dm}$. We notice that $w_{\rm dm0}$ and $w_{\rm dm1}$ are equally preferred/constrained by the considered data in the order of magnitude. In other words, the presence of $w_{\rm dm1}$ is not neglected by the data in comparison to the $w_{\rm dm} = \rm constant$ case. The parameter $w_{\rm dm1}$ shows correlation with other parameters similar to $w_{\rm dm0}$, as may be seen in Figures 4.1 and 4.3. The presence of $w_{\rm dm1}$ minimally relaxes the constraints on the full model baseline parametric space in comparison to the $w_{\rm dm} = \rm constant$ case in earlier studies.

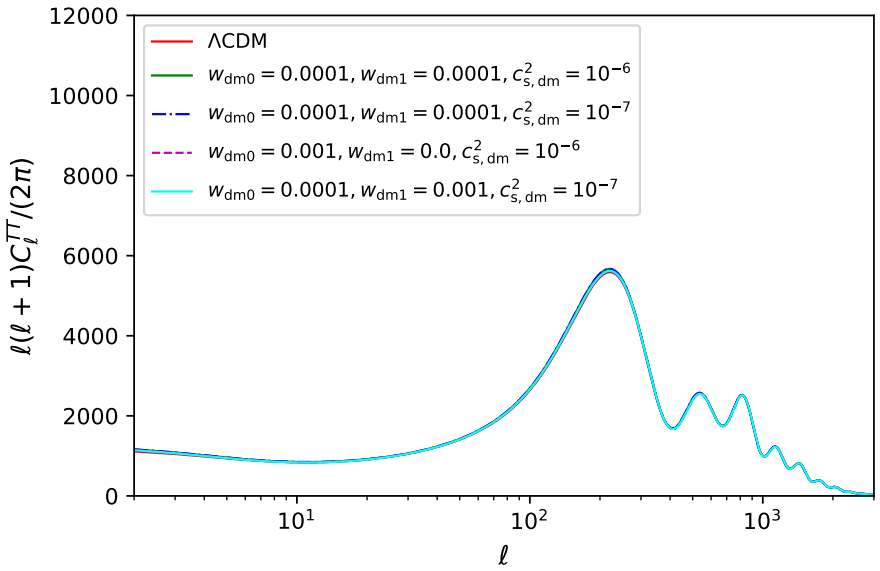

Figure 4.5: The CMB TT power spectra from base line Planck 2015 ΛCDM model for some values of model parameters as mentioned in the legend while other relevant parameters are fixed to their mean value as shown in Table 4.2.

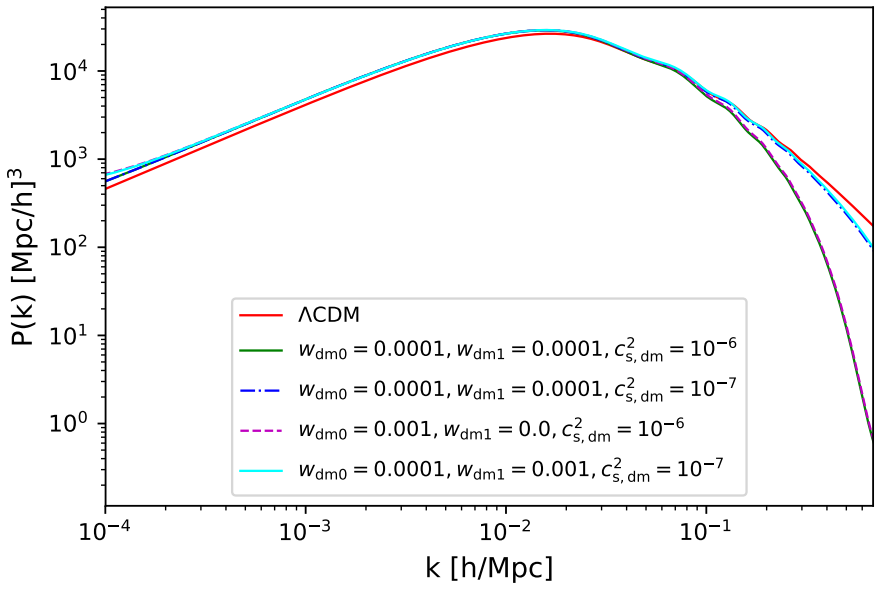

Figure 4.6: The matter power spectra from baseline Planck 2015 ΛCDM model for some values of model parameters as mentioned in the legend while other relevant parameters are fixed to their mean value as shown in Table 4.2.

4.2.4 Effects on CMB TT and matter power spectra

In this study, we have considered the possibility of $w_{\rm dm} > 0$. It should generate similar effects on CMB TT to that when considering changes over $\omega_{\rm dm}$ (dimensionless DM density), modifying the heights of the first few acoustic peaks. In fact, $w_{\rm dm} > 0$ should increase the DM density at the time of radiation-matter equality and, therefore modify the modes that enter the horizon during radiation domination, leading to suppression around the acoustic peak scales. Also, the acoustic peaks in the CMB depend on the angular diameter distance to the last scattering, where it is influenced by the change in the expansion rate of H, which is modified here by the presence of the dynamical $w_{\rm dm}$ term. As $w_{\rm dm}$ increases, the angular diameter distance to the last scattering surface decreases such that features are shifted to smaller angular scales. Larger values for $w_{\rm dm}$ would result in behaving more like radiation for DM, generating large acoustic driving and boosting on the CMB peaks, with prevision that should be inconsistent with observations. Also, the major indirect evidence for DM comes from the CMB peaks. The possible absence of CDM particles would introduce large acoustic driving, boosting the peak amplitude, which can also lead to a spectrum that completely disagrees with observations. That is why when considering data from CMB, in general, very strong limits like $w_{\rm dm} \ll 1$ are observed. The effective sound speed $\hat{c}^2_{\rm s,dm}$ parameter will influence the spectrum on acoustic peak similar to $w_{\rm dm}$, where $\hat{c}^2_{\rm s,dm} > 0$ would cause the amplitude of the acoustic peaks to decrease relative to the large scale anisotropy. At large scales, where the integrated Sachs-Wolfe effect is predominant, the main effect of $\hat{c}^2_{\rm s,dm} > 0$ is to increase the gravitational potential decay after recombination until the present time, causing an increase to the anisotropy for $l < 40$. Changing $w_{\rm dm} > 0$ has a very mild effect on the integrated Sachs-Wolfe, compared to $\hat{c}^2_{\rm s,dm}$, but both parameters with positive variation yield the same effects on large scales. Figure 4.5 shows how the parameters, $w_{\rm dm0}$, $w_{\rm dm1}$ and $\hat{c}^2_{s,\rm dm}$ can affect the CMB TT spectrum. We note small and significant deviations on the minimal ΛCDM model as described above, where the effects on the acoustic peaks (i.e., effects for $l > 50$) are less noticeable. Possible effects to shift the spectrum into the

Table 4.4: Difference of AIC values of ΛWDM model under consideration with respect to ΛCDM model (reference model) with four data combinations.

Data	$\Delta\mathrm{AIC}_{\Lambda\mathrm{WDM}}$
CMB	7.78
CMB + BAO	5.52
CMB + HST	2.62
CMB + BAO + HST	2.10

direction to smaller angular scales are minimal due to very small corrections (insignificant corrections) on the angular diameter distance at last scattering as the effects of $w_{\rm dm0}$, $w_{\rm dm1} \ll 1$ are very small. On the other hand, the LSS of the Universe also depends directly on the DM properties. As pointed out in [166], the clustering scale becomes independent of the DM EoS, and DM extended properties should change only the amplitude of the perturbations, that can be observed by looking at the matter power spectrum. We also expect these changes basically to be in the order of magnitude compatible with the observed Universe. Therefore, we set the free parameters within the limits derived here up to 99% CL. The presence of $\hat{c}^2_{\rm s,dm} > 0$ decreases the amplitude on $P(k)$, and in return $w_{\rm dm0} > 0$ increases the amplitude of perturbations. Figure 4.6 shows $P(k, z = 0)$ for some selected values of $\hat{c}^2_{\rm s,dm}$, $w_{\rm dm0}$ and $w_{\rm dm1}$. In general, we notice that $w_{\rm dm0}$ influences more the amplitude than $\hat{c}^2_{\rm s,dm}$, causing a net increase in the amplitude of the matter power spectrum.

4.2.5 Bayesian model comparison

In the present work, we have analyzed an extension of the standard ΛCDM model. Thus, apart from parameter estimation performed here, it is important to perform a statistical comparison of the considered model with a well-fitted standard model (reference model). For this purpose, we use information criterion AIC [68, 69] as discussed in subsection 2.1.4 of Chapter 2.

Table 4.4 summarizes the $\Delta\mathrm{AIC}$ values of the considered model for all the data combinations. We have $\Delta\mathrm{AIC}$ values greater than the threshold value for the data: CMB and CMB + BAO. Therefore, it can be claimed that the standard ΛCDM model is strongly

favored over the ΛWDM model with data combinations: CMB and CMB + BAO. On another hand, for CMB + HST and CMB + BAO + HST combinations, we can not claim statistical evidence in favor of either of models since $\Delta\mathrm{AIC}$ values are much less than the threshold value.

4.2.6 Constraints on the extended DM properties with variable dark energy

This subsection describes the results on extended DM properties with a time-varying DE via the CPL parametrization given below:

$$w_{\rm de} = w_{\rm de0} + (1-a)w_{\rm de1}, \tag{4.17}$$

where the constant parameters $w_{\rm de0}$ and $w_{\rm de1}$ are to be constrained by the observational data. The conservation equation for a time-varying dark energy EoS reads as

$$\dot{\rho}_{\rm de} + 3\frac{\dot{a}}{a}(1+w_{\rm de})\rho_{\rm de} = 0. \tag{4.18}$$

Using the eqs. (4.17) and (4.18), the evolution for dark energy density is given as

$$\rho_{\rm de} = \rho_{\rm de0}\, a^{-3(1+w_{\rm de0}+w_{\rm de1})}\, e^{-3w_{\rm de1}(1-a)}. \tag{4.19}$$

This is the additional equation for this study in addition to eq. (4.5). The main motive of this study is to see possible effects of the time-varying DE on extended DM parameters as well as on other various model parameters. The parametric space of VWDM model is given by:

$$\mathcal{P}_{\rm VWDM} = \Big\{\omega_{\rm b},\, \omega_{\rm dm},\, \theta_s,\, A_s,\, n_s,\, \tau_{\rm reio},\, w_{\rm dm0},\, w_{\rm dm1},\, \hat{c}^2_{\rm s,dm}\, w_{\rm de0},\, w_{\rm de1}\Big\},$$

To show the consistency and to make the results comparable with the first study with cosmological constant type DE, we have employed the same sets of data combinations

for this case also. We have used the flat priors on parameters as mentioned in Table 4.1 together with the priors: $-2.5 \leq w_{\rm de0} \leq 0.5$ and $-2.0 \leq w_{\rm de1} \leq 2.0$, on DE EoS parameters. Table 4.5 represents the statistical bounds on the free parameters and some derived parameters of VWDM model with four data combinations: CMB, CMB + BAO, CMB + HST, and CMB + BAO + HST, as used in first study. The constraints on the baseline (first six) parameters of ΛCDM model are in agreement with the constraints obtained in our first study with little deviations with some data combinations. For instance, abundance of physical DM density $\Omega_{\rm dm}$ is significantly less with the combinations: CMB + BAO and CMB + HST as compared to our first study. It is observed that (see Tables 4.2 and 4.5) with the first three data combinations, a time-varying DE allows very less amount of DM density in the presence of extended DM parameters as compared to ΛCDM model. From

Table 4.5: Constraints on the free parameters and some derived parameters of the VWDM model for four different data combinations. The upper and lower values over the mean value of each parameter denote 68% CL and 95% CL errors. For the parameters: $w_{\rm dm0}$, $w_{\rm dm1}$, and $\hat{c}^2_{\rm s,dm}$, the upper bounds at 95% CL are mentioned. The parameter H_0 is measured in the units of km s^{-1} Mpc^{-1}. The $\chi^2_{\rm min}$ values are displayed in the last row.

Parameter	CMB	CMB + BAO	CMB + HST	CMB + BAO + HST
$10^2\omega_{\rm b}$	$2.217^{+0.017+0.033}_{-0.017-0.031}$	$2.217^{+0.017+0.033}_{-0.017-0.035}$	$2.218^{+0.016+0.032}_{-0.016-0.032}$	$2.216^{+0.015+0.030}_{-0.015-0.029}$
$\omega_{\rm dm}$	$0.1154^{+0.0029+0.0047}_{-0.0022-0.0054}$	$0.1162^{+0.0020+0.0037}_{-0.0020-0.0039}$	$0.1157^{+0.0026+0.0046}_{-0.0022-0.0048}$	$0.1171^{+0.0019+0.0033}_{-0.0017-0.0036}$
$100\theta_s$	$1.04172^{+0.00031+0.00060}_{-0.00031-0.00057}$	$1.04172^{+0.00035+0.00060}_{-0.00030-0.00066}$	$1.04172^{+0.00032+0.00062}_{-0.00032-0.00059}$	$1.04171^{+0.00030+0.00061}_{-0.00030-0.00059}$
$\ln 10^{10} A_s$	$3.071^{+0.030+0.066}_{-0.035-0.062}$	$3.092^{+0.030+0.058}_{-0.030-0.058}$	$3.081^{+0.030+0.060}_{-0.030-0.056}$	$3.085^{+0.028+0.057}_{-0.028-0.055}$
n_s	$0.9651^{+0.0050+0.0110}_{-0.0055-0.0099}$	$0.9653^{+0.0048+0.0098}_{-0.0048-0.0089}$	$0.9653^{+0.0051+0.0097}_{-0.0051-0.0010}$	$0.9638^{+0.0044+0.0088}_{-0.0044-0.0084}$
$\tau_{\rm reio}$	$0.067^{+0.015+0.034}_{-0.018-0.032}$	$0.077^{+0.016+0.031}_{-0.016-0.031}$	$0.072^{+0.015+0.031}_{-0.015-0.030}$	$0.074^{+0.015+0.029}_{-0.015-0.029}$
$w_{\rm dm0}$ (95% CL)	$< 2.38 \times 10^{-3}$	$< 1.90 \times 10^{-3}$	$< 2.36 \times 10^{-3}$	$< 1.78 \times 10^{-3}$
$w_{\rm dm1}$ (95% CL)	$< 2.88 \times 10^{-3}$	$< 2.08 \times 10^{-3}$	$< 2.38 \times 10^{-3}$	$< 1.77 \times 10^{-3}$
$\hat{c}^2_{\rm s,dm}$ (95% CL)	$< 2.38 \times 10^{-6}$	$< 2.05 \times 10^{-6}$	$< 2.27 \times 10^{-6}$	$< 2.28 \times 10^{-6}$
$w_{\rm de0}$	$-1.64^{+0.41+1.10}_{-0.71-0.91}$	$-0.80^{+0.15+0.51}_{-0.29-0.34}$	$-0.91^{+0.29+0.41}_{-0.19-0.48}$	$-1.13^{+0.14+0.28}_{-0.14-0.27}$
$w_{\rm de1}$	$-0.26^{+0.97+1.80}_{-1.20-1.80}$	$-0.42^{+0.63+0.85}_{-0.37-1.40}$	$-0.72^{+0.69+1.60}_{-1.20-1.30}$	$0.24^{+0.47+0.80}_{-0.37-0.87}$
$\Omega_{\rm m}$	$0.165^{+0.033+0.160}_{-0.094-0.110}$	$0.310^{+0.017+0.053}_{-0.031-0.042}$	$0.258^{+0.012+0.026}_{-0.013-0.024}$	$0.275^{+0.011+0.024}_{-0.013-0.022}$
H_0	$99.0^{+20.0+40.0}_{-30.0-40.0}$	$67.1^{+3.0+4.7}_{-2.3-5.3}$	$73.4^{+1.7+3.3}_{-1.7-3.3}$	$71.3^{+1.5+3.0}_{-1.5-2.9}$
σ_8	$0.830^{+0.120+0.330}_{-0.160-0.280}$	$0.732^{+0.085+0.110}_{-0.044-0.150}$	$0.754^{+0.110+0.140}_{-0.047-0.170}$	$0.752^{+0.099+0.120}_{-0.049-0.150}$
$\chi^2_{\rm min}/2$	6476.15	6480.61	6476.11	6483.09

Table 4.5, it can be seen that the constraints on both the DM EoS parameters are of order 10^{-3} at 95% CL with all data combinations. In this analysis, the tighter upper bounds

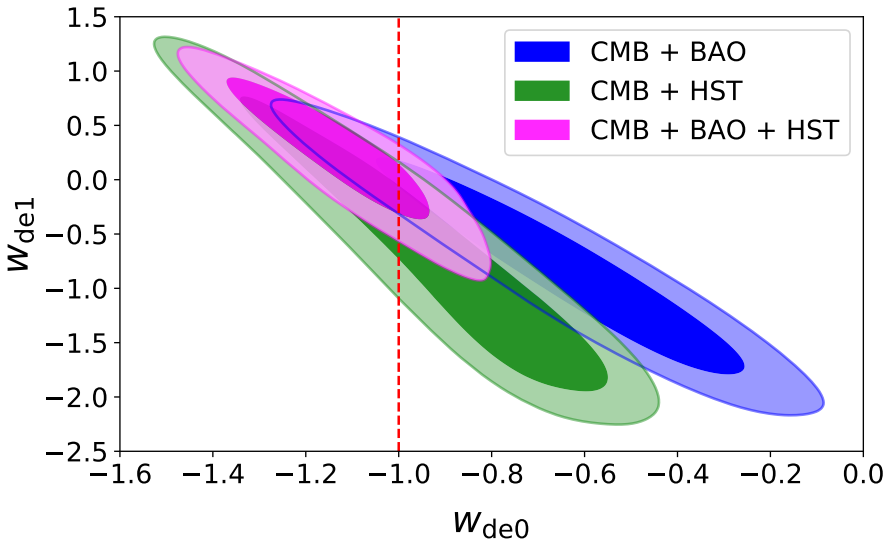

Figure 4.7: Confidence contours (68% and 95% CL) in $w_{\rm de0} - w_{\rm de1}$ plane from data combinations mentioned in the legend. The contour plot with CMB data is not shown due to the large errors on both the parameters.

on DM EoS parameters: $w_{\rm dm0}$, $w_{\rm dm1}$ are 1.78×10^{-3} and 1.77×10^{-3}, respectively, at 95% CL. Both are obtained with combined data set: CMB + BAO + HST. We have obtained the constraints on sound speed, $\hat{c}^2_{\rm s,dm}$ of DM of order 10^{-6} at 95% CL with all data combinations used here. Therefore, we notice that the constraints on extended DM parameters are similar in order of magnitude to those found in our first analysis where a cosmological constant type DE was assumed. Thus, the time-varying DE does not affect the extended DM parameters. A clear indication of phantom behaviour of DE is observed from CMB alone and from joint analysis with constraints: $w_{\rm de0} = -1.64^{+0.41}_{-0.71}$ and $w_{\rm de0} = -1.13 \pm 0.14$ both at 68% CL, respectively. However, with other two data combinations a quintessence behavior of DE is observed. Also, see the two dimensional marginalized contours in Figure 4.7, where the vertical dotted line corresponds to a cosmological constant form of DE, i.e., $w_{\rm de0} = -1$. We have not shown $w_{\rm de0} - w_{\rm de1}$ plane for CMB data because of large errors on both the DE EoS parameters. Figure 4.8 represents the parametric space in the plane $\sigma_8 - H_0$ for VWDM model with three data combinations. We have large mean value of Hubble constant from CMB data alone which is due to large number of parameters in the model. So CMB data alone are not able to constrain it

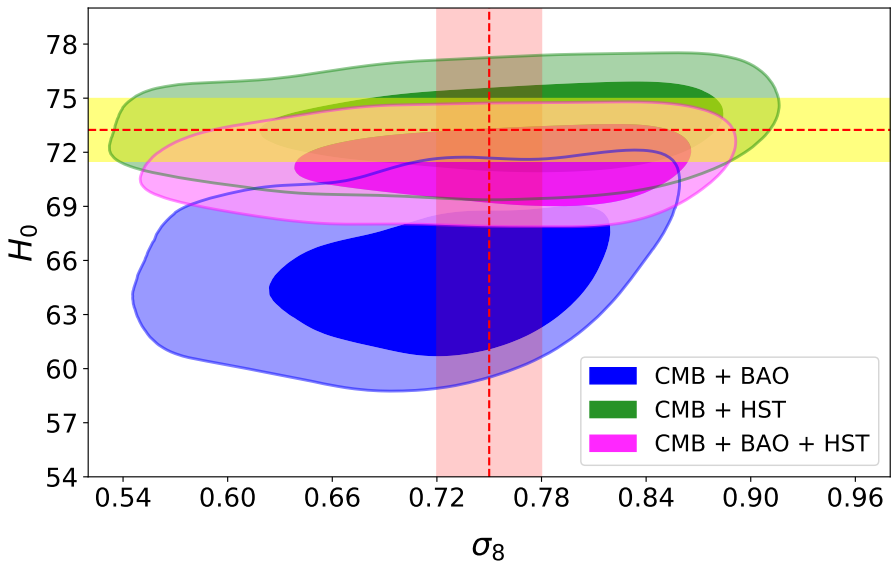

Figure 4.8: Parametric space in the plane $H_0 - \sigma_8$ for VWDM model from three different data combinations. The horizontal yellow band corresponds to $H_0 = 73.24 \pm 1.74$ km $s^{-1}Mpc^{-1}$ from local measurement whereas the vertical light red band corresponds to $\sigma_8 = 0.75 \pm 0.03$ from Planck-SZ measurement. The contour plot with CMB data is not shown due the large errors on both the parameters.

well. We observe that the inclusion of HST prior in the analysis leads to higher values of Hubble constant H_0, consistent with local measurements. With CMB + BAO dataset, H_0 is consistent with Planck CMB measurements. The present DE EoS $w_{\rm de0}$ finds a negative correlation with the Hubble constant, (see Figure 4.9. We have not shown the contour plot with CMB data due to the large errors on H_0, but the correlation of H_0 with $w_{\rm de0}$ is same with this CMB data also. In this study, we also have significantly lower values of σ_8 with all data combinations except with CMB alone in which case it is consistent with the Planck measurement with large errors. With other combinations, the values of σ_8 obtained here are consistent with our first case favoring to LSS measurements. See Figure 4.8, where the range of σ_8 from Planck-SZ measurement is shown in vertical light red band. Thus, the constraints on σ_8 parameter have not changed with the time-varying DE except with CMB data alone. The parameter σ_8 finds a negative correlation with sound speed of DM as shown in Figure 4.10, where the trend is same as in the first study with all data combinations.

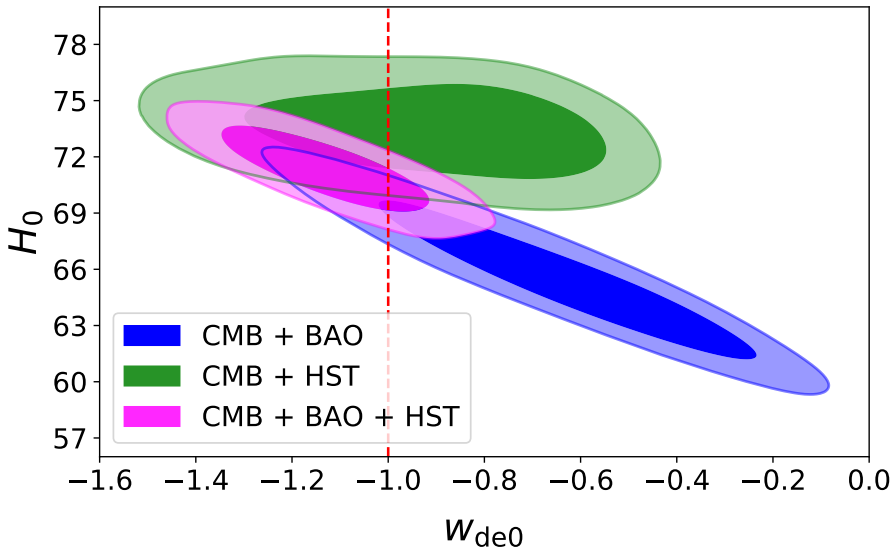

Figure 4.9: 68% and 95% confidence contours in $w_{\rm de0} - H_0$ plane from data combinations mentioned in legend. The contour plot with CMB data is not shown to the large errors on both the parameters.

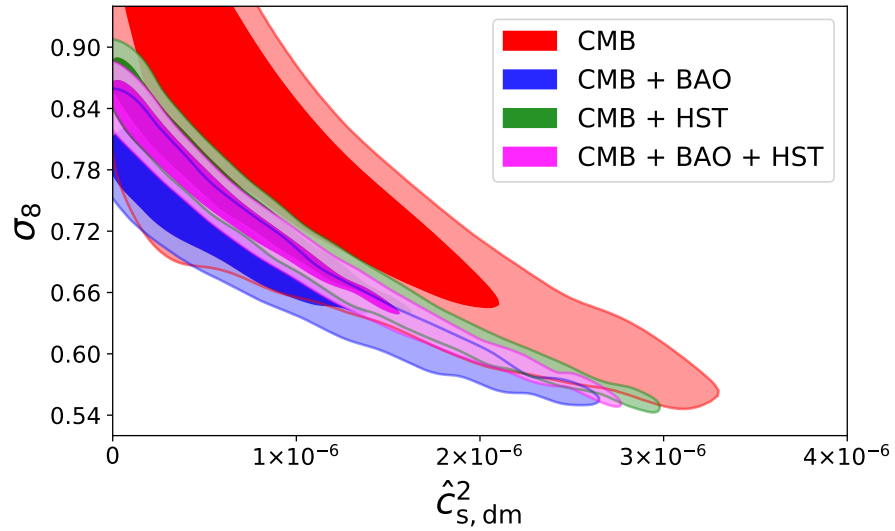

Figure 4.10: Parametric space in the plane $\hat{c}^2_{\rm s,dm} - \sigma_8$ with all data combinations for VWDM model.

4.3 Concluding remarks

The presence of DM plays a crucial role in explaining the current cosmological data wherein it is almost impossible to explain the origin of CMB and LSS without the presence of this dark component. Despite being a key ingredient in modern cosmology, the nature of DM is one of the most open questions in contemporary science, and its general properties like spin, mass, interaction cross-section, lifetime, etc, are not yet completely closed for study via phenomenological attempts. In this chapter, we have investigated an extension of the ΛCDM model via the extended properties of DM: a possible time dependence of EoS of DM via the CPL parametrization and the constant non-null sound speed. We have derived new and robust constraints on the extended free parameters of DM and DE. In our first study, the most tight constraints are imposed by CMB + BAO data where the three parameters $w_{\rm dm0}$, $w_{\rm dm1}$ and $\hat{c}^2_{\rm s,dm}$ are respectively constrained to be less than 1.43×10^{-3}, 1.44×10^{-3} and 1.79×10^{-6} at 95% CL (see Table 4.2), which are in line with the results in the literature. Thus, the extended parameters of DM are strongly constrained, and all show consistency with zero at 95% CL, indicating no evidence beyond the CDM paradigm. Further, the extended properties of DM significantly affect several parameters of the base ΛCDM model. In particular, with all data combinations, we have found significantly larger mean values of H_0 and lower mean values of σ_8 in comparison to the base ΛCDM model. Thus, the well-known H_0 and σ_8 tensions might be reconciled in the presence of extended DM parameters within the ΛCDM framework. In the first study, we have also estimated the warmness of DM particles as well as its mass scale, and find a lower bound: $\sim$ 500 eV from our analyses, compatible with the Tremaine-Gunn bound and other such limits found in the literature. In the second study with the time-variable DE EoS parameter, we have found similar constraints in order of magnitude on all extended parameters of DM. Thus, we observed that the time-varying DE does not affect the extended DM parameters. In this case, the tight constraints on DM EoS parameters are obtained with CMB + BAO + HST: $w_{\rm dm0} < 1.78 \times 10^{-3}$ and $w_{\rm dm1} < 1.77 \times 10^{-3}$, both at at 95% CL. The tightest constraint on sound speed of DM

is obtained to be less than 2.05×10^{-6} with CMB + BAO (see Table 4.5). With some data combinations, DE shows phantom behaviour whereas with others it is quintessence. From our analyzes, it is clear that even a little deviation provided by the extended DM properties could lead to interesting, useful and significant changes in the evolution of the base ΛCDM Universe. So it would be worthwhile to investigate extended DM properties in the light of forthcoming data from various surveys/experiments in the near future.